



# Nearly diffraction limited FTIR mapping using an ultrastable broadband femtosecond laser tunable from 1.33 to 8 $\mu\text{m}$

FLORIAN MÖRZ,<sup>1,\*</sup> ROSTYSLAV SEMENYSHYN,<sup>1</sup> TOBIAS STEINLE,<sup>1</sup> FRANK NEUBRECH,<sup>1,3</sup> UTE ZSCHIESCHANG,<sup>2</sup> HAGEN KLAUK,<sup>2</sup> ANDY STEINMANN,<sup>1</sup> AND HARALD GIESSEN<sup>1</sup>

<sup>1</sup>4<sup>th</sup> Physics Institute, University of Stuttgart, Research Center SCoPE, Germany

<sup>2</sup>Max Planck Institute for Solid State Research, Stuttgart, Germany

<sup>3</sup>Kirchhoff-Institute for Physics, University Heidelberg, Im Neuenheimer Feld 227, 69120 Heidelberg, Germany

\*f.moerz@pi4.uni-stuttgart.de

**Abstract:** Micro-Fourier-transform infrared (FTIR) spectroscopy is a widespread technique that enables broadband measurements of infrared active molecular vibrations at high sensitivity. SiC globars are often applied as light sources in tabletop systems, typically covering a spectral range from about 1 to 20  $\mu\text{m}$  (10 000 – 500  $\text{cm}^{-1}$ ) in FTIR spectrometers. However, measuring sample areas below 40x40  $\mu\text{m}^2$  requires very long integration times due to their inherently low brilliance. This hampers the detection of ultrasmall samples, such as minute amounts of molecules or single nanoparticles. In this publication we extend the current limits of FTIR spectroscopy in terms of measurable sample areas, detection limit and speed by utilizing a broadband, tabletop laser system with MHz repetition rate and femtosecond pulse duration that covers the spectral region between 1250 – 7520  $\text{cm}^{-1}$  (1.33 – 8  $\mu\text{m}$ ). We demonstrate mapping of a 150x150  $\mu\text{m}^2$  sample of 100 nm thick molecule layers at 1430  $\text{cm}^{-1}$  (7  $\mu\text{m}$ ) with 10x10  $\mu\text{m}^2$  spatial resolution and a scan speed of 3.5  $\mu\text{m}/\text{sec}$ . Compared to a similar globar measurement an order of magnitude lower noise is achieved, due to an excellent long-term wavelength and power stability, as well as an orders of magnitude higher brilliance.

© 2017 Optical Society of America under the terms of the [OSA Open Access Publishing Agreement](#)

**OCIS codes:** (190.4970) Parametric oscillators and amplifiers; (300.6300) Spectroscopy, Fourier transforms; (300.6360) Spectroscopy, laser.

## References and links

1. P. B. Fellgett, "On the ultimate sensitivity and practical performance of radiation detectors," *J. Opt. Soc. Am.* **39**(11), 970–976 (1949).
2. P. Connes, "Astronomical Fourier Spectroscopy," *Annu. Rev. Astron. Astrophys.* **8**(1), 209–230 (1970).
3. P. Jacquinet, "New developments in interference spectroscopy," *Rep. Prog. Phys.* **23**(1), 267–312 (1960).
4. P. R. Griffiths and J. A. de Haseth, *Fourier Transform Infrared Spectroscopy* (Wiley, 2007), Chap. 14.
5. R. Gasper, T. Mijatovic, R. Kiss, and E. Goormaghtigh, "FTIR spectroscopy reveals the concentration dependence of cellular modifications induced by anticancer drugs," *Spectroscopy (Springf.)* **24**(1-2), 45–49 (2010).
6. C. Petibois and G. Dél  ris, "Chemical mapping of tumor progression by FT-IR imaging: towards molecular histopathology," *Trends Biotechnol.* **24**(10), 455–462 (2006).
7. A. Barth, "Infrared spectroscopy of proteins," *Biochim. Biophys. Acta* **1767**(9), 1073–1101 (2007).
8. C. Petibois, G. Deleris, M. Piccinini, M. Cestelli-Guidi, and A. Marcelli, "A bright future for synchrotron imaging," *Nat. Photonics* **3**(4), 179 (2009).
9. M. Martin, U. Schade, P. Lerch, and P. Dumas, "Recent applications and current trends in analytical chemistry using synchrotron-based Fourier-transform infrared microspectroscopy," *Trends Analyt. Chem.* **29**(6), 453–463 (2010).
10. T. Steinle, F. Neubrech, A. Steinmann, X. Yin, and H. Giessen, "Mid-infrared Fourier-transform spectroscopy with a high-brilliance tunable laser source: investigating sample areas down to 5  $\mu\text{m}$  diameter," *Opt. Express* **23**(9), 11105–11113 (2015).

11. I. W. Levin and R. Bhargava, "Fourier Transform Infrared Vibrational Spectroscopic Imaging: Integrating Microscopy and Molecular Recognition," *Annu. Rev. Phys. Chem.* **56**(1), 429–474 (2005).
12. R. F. Curl, F. Capasso, C. Gmachl, A. A. Kosterev, B. McManus, R. Lewicki, M. Pusharsky, G. Wysocki, and F. K. Tittel, "Quantum cascade lasers in chemical physics," *Chem. Phys. Lett.* **487**(1-3), 1–18 (2010).
13. A. Hasenkampf, N. Kröger, A. Schönhal, W. Petrich, and A. Pucci, "Surface-enhanced mid-infrared spectroscopy using a quantum cascade laser," *Opt. Express* **23**(5), 5670–5680 (2015).
14. J. Mandon, G. Guelachvili, and N. Picqué, "Fourier transform spectroscopy with a laser frequency comb," *Nat. Photonics* **3**(2), 99–102 (2009).
15. I. Coddington, N. Newbury, and W. Swann, "Dual-comb spectroscopy," *Optica* **3**(4), 414–426 (2016).
16. L. Maidment, P. G. Schunemann, and D. T. Reid, "Molecular fingerprint-region spectroscopy from 5 to 12  $\mu\text{m}$  using an orientation-patterned gallium phosphide optical parametric oscillator," *Opt. Lett.* **41**(18), 4261–4264 (2016).
17. S. Chaitanya Kumar, J. Krauth, A. Steinmann, K. T. Zawilski, P. G. Schunemann, H. Giessen, and M. Ebrahim-Zadeh, "High-power femtosecond mid-infrared optical parametric oscillator at 7  $\mu\text{m}$  based on CdSiP<sub>2</sub>," *Opt. Lett.* **40**(7), 1398–1401 (2015).
18. T. Südmeyer, J. Aus der Au, R. Paschotta, U. Keller, P. G. Smith, G. W. Ross, and D. C. Hanna, "Femtosecond fiber-feedback optical parametric oscillator," *Opt. Lett.* **26**(5), 304–306 (2001).
19. T. Steinle, A. Steinmann, R. Hegenbarth, and H. Giessen, "Watt-level optical parametric amplifier at 42 MHz tunable from 1.35 to 4.5  $\mu\text{m}$  coherently seeded with solitons," *Opt. Express* **22**(8), 9567–9573 (2014).
20. H. Linnenbank and S. Linden, "High repetition rate femtosecond double pass optical parametric generator with more than 2 W tunable output in the NIR," *Opt. Express* **22**(15), 18072–18077 (2014).
21. J. Krauth, T. Steinle, B. Liu, M. Floess, H. Linnenbank, A. Steinmann, and H. Giessen, "Low drift cw-seeded high-repetition-rate optical parametric amplifier for fingerprint coherent Raman spectroscopy," *Opt. Express* **24**(19), 22296–22302 (2016).
22. F. Mörz, T. Steinle, A. Steinmann, and H. Giessen, "Multi-Watt femtosecond optical parametric master oscillator power amplifier at 43 MHz," *Opt. Express* **23**(18), 23960–23967 (2015).
23. T. Steinle, F. Mörz, A. Steinmann, and H. Giessen, "Ultra-stable high average power femtosecond laser system tunable from 1.33 to 20  $\mu\text{m}$ ," *Opt. Lett.* **41**(21), 4863–4866 (2016).
24. L. Kühner, M. Hentschel, U. Zschieschang, H. Klauk, J. Vogt, C. Huck, H. Giessen, and F. Neubrech, "Nanoantenna-Enhanced Infrared Spectroscopic Chemical Imaging," *ACS Sens.* **2**(5), 655–662 (2017).
25. T. Neuman, C. Huck, J. Vogt, F. Neubrech, R. Hillenbrand, J. Aizpurua, and A. Pucci, "Importance of Plasmonic Scattering for an Optimal Enhancement of Vibrational Absorption in SEIRA with Linear Metallic Antennas," *J. Phys. Chem. C* **119**(47), 26652–26662 (2015).
26. F. Neubrech, C. Huck, K. Weber, A. Pucci, and H. Giessen, "Surface-Enhanced Infrared Spectroscopy Using Resonant Nanoantennas," *Chem. Rev.* **117**(7), 5110–5145 (2017).
27. S. Amarie, T. Ganz, and F. Keilmann, "Mid-infrared near-field spectroscopy," *Opt. Express* **17**(24), 21794–21801 (2009).
28. F. Huth, M. Schnell, J. Wittborn, N. Ocelic, and R. Hillenbrand, "Infrared-spectroscopic nanoimaging with a thermal source," *Nat. Mater.* **10**(5), 352–356 (2011).
29. S. Bensmann, F. Gaußmann, M. Lewin, J. Wüppen, S. Nyga, C. Janzen, B. Jungbluth, and T. Taubner, "Near-field imaging and spectroscopy of locally strained GaN using an IR broadband laser," *Opt. Express* **22**(19), 22369–22381 (2014).

## 1. Introduction

Fourier-transform infrared spectroscopy (FTIR) is a frequently used technique to investigate molecular vibrations, as it provides an increased sensitivity and signal-to-noise ratio (SNR) (Felgett advantage [1]), a higher spectral accuracy (Connes advantage [2]), and a higher optical throughput (Jacquinot advantage [3]) compared to conventional dispersive spectrometers. In micro-FTIR spectroscopy [4] an optical microscope is attached to a FTIR spectrometer. This allows tighter focusing, spatially resolved measurements, and scanning. Hence, compared to conventional FTIR spectroscopy smaller structures or less concentrated molecular solutions can be investigated. This method has found many applications such as the determination of molecular structures and concentrations [5], cancer detection [6], or protein sensing [7].

In order to cover a broad spectral range, state-of-the-art light sources are thermal in nature such as globars, or synchrotrons [8, 9]. Both allow investigating vibrational resonances between 500 – 10 000  $\text{cm}^{-1}$  (1 – 20  $\mu\text{m}$ ), where the upper spectral limit is determined by optics of the FTIR spectrometer and the detectors. They are the best choice if samples need to be characterized over a broad spectral range. However, if very small samples such as single nanoparticles need to be investigated, the noise strongly increases using globars. This can be

explained by their low brilliance, which is defined as the number of photons per second, per unit source area, per unit solid angle and per 0.1% bandwidth of the central frequency. Globars typically reach a brilliance on the order of  $10^{15}$  ph/s/mm<sup>2</sup>/sr/0.1%BW, whereas synchrotrons already reach an about 2-3 orders of magnitude higher brilliance [8, 10]. It has been shown in [10] that the minimum area that can be measured on reasonable timescales employing a globar is on the order of  $40 \times 40 \mu\text{m}^2$ , below the signal-to-noise ratio strongly decreases. Measuring smaller areas can be achieved by using longer integration times and higher averaging, which easily leads to extremely long measurement times. To conduct spectroscopic measurements which include spatial information of the sample or spectroscopy of very low sample concentrations in an acceptable measurement time, light sources exhibiting a higher brilliance are required. Therefore synchrotrons have been recommended for FTIR mapping [11]. Furthermore, they are very suitable due to their broad bandwidth and noise characteristics. However, the available measurement time is usually limited and associated with high costs. Alternative tabletop light sources for FTIR spectroscopy are laser sources due to an up to 4 orders of magnitude higher brilliance compared to synchrotrons, as shown in [10], where a similar light source as ours has been used. Available laser sources for tabletop setups are often based on quantum cascade lasers (QCLs) [12, 13]. These lasers typically exhibit a very narrow linewidth of  $1 \text{ cm}^{-1}$  but provide a high brilliance and good noise characteristics. In general, QCLs are available between  $770 - 2500 \text{ cm}^{-1}$  ( $4 - 13 \mu\text{m}$ ), however at a limited tuning range of  $1 - 2 \mu\text{m}$ . Therefore, commercial systems often consist of several laser modules to cover a reasonable wavelength range. In consequence, QCLs are highly suited for imaging applications at a certain frequency, whereas measuring complete vibrational spectra requires elaborate stitching methods, due to their narrow linewidth. Furthermore, QCLs are typically operated at kHz repetition rates and nanosecond pulse durations. Another technique that provides a broadband laser source and has been successfully applied to FTIR spectroscopy is the generation of frequency combs [14, 15]. This allows measurements at a very high sensitivity, high spectral resolution, and a broad bandwidth. However, it also requires sophisticated detection techniques as well as electronics, and the available spectral range shows a gap between roughly  $3 - 7 \mu\text{m}$  [15]. Unfortunately, frequency comb spectroscopy is difficult to combine with commercially available FTIR spectrometers. Other laser sources, exhibiting a high brilliance, are based on optical parametric oscillators (OPOs) [16, 17], as a broad wavelength range can be covered. However, they are highly sensitive to ambient conditions and require external wavelength and power stabilization to obtain sufficient noise levels.

Here, we employ a fiber-feedback OPO (ffOPO) [18] that overcomes these issues, as most of the cavity is transferred into a single mode fiber. By amplifying the ffOPO output with an optical parametric amplifier (OPA) and converting the light to the mid-IR using difference frequency generation (DFG), a tabletop light source is realized that exceeds the bandwidth of QCLs by two orders of magnitude and exhibits excellent long-term wavelength and power stability. Furthermore it covers a total tuning range that is difficult to cover with QCLs. In contrast to the system presented in [10] our system also covers the mid-IR spectral range and exhibits a broader bandwidth. Previous approaches in our group were based on soliton-seeded OPAs [19], optical parametric generation [20], or cw-seeded double pass OPAs [21]. However, the noise level of the setup presented in this publication is minimum, which is crucial for FTIR spectroscopy. We demonstrate the performance of our system by conducting a  $150 \times 150 \mu\text{m}^2$  map of several 100 nm thick molecular layers at around  $1430 \text{ cm}^{-1}$  ( $7 \mu\text{m}$ ) at  $10 \times 10 \mu\text{m}^2$  spatial resolution. To demonstrate the improved detection limit molecular vibrations exhibiting absorptions on the order of 2% and smaller are detected. We refer to the smallest signal that can be measured at a reasonable precision for a given measurement procedure as the detection limit. Thus the signal-to-noise ratio contributes to this limit and two measurements that might have the same sensitivity can have different detection limits.

All measurements in this publication are conducted with our laser system and with a global to compare the laser performance to the most common tabletop FTIR light source.

## 2. Experimental setup

The main part of the light source is a fiber-feedback OPO that seeds an optical parametric amplifier. As depicted in Fig. 1, both the OPO and the OPA are synchronously pumped by an Yb solid-state oscillator. A detailed description of a similar system has been presented in [22]. In contrast to [22], a commercially available Yb solid-state laser by Montfort GmbH, with much shorter pulses and hence, much broader bandwidth, is applied as a pump source in the presented system. It provides 98 fs pulses at 73 MHz repetition rate and a central wavelength of 1.048  $\mu\text{m}$ . The total average output power is on the order of 2.5 W, from which 1 W is used to pump the ffOPO and 1.5 W is used to pump the OPA. Thus, the laser wavelength can be tuned nearly gap-free between 1.33 and 4.6  $\mu\text{m}$  (2174 – 7520  $\text{cm}^{-1}$ ). Then, the OPA signal and idler beams are combined in a 2-mm-long AR-coated AgGaSe<sub>2</sub> crystal to generate their difference frequency. Due to a higher nonlinearity below 8  $\mu\text{m}$  wavelength, type 1 angular phase-matching is used. More details concerning the laser setup can be found in [23], where we demonstrated a tuning range spanning from 1.33 – 20  $\mu\text{m}$  wavelength (500 – 7520  $\text{cm}^{-1}$ ). In contrast to [23], the tuning range of this setup is limited to 8  $\mu\text{m}$  (1250  $\text{cm}^{-1}$ ), due to a roughly 3 times lower pump power. However, this system exhibits an increased bandwidth, shorter pulses and a higher repetition rate. Figure 2 depicts the DFG tuning range, reaching from 4.65 to 8  $\mu\text{m}$  (1250 – 2150  $\text{cm}^{-1}$ ) with a FWHM of at least 250 nm. Up to 2.65 mW output power are measured at 5.5  $\mu\text{m}$  wavelength (1818  $\text{cm}^{-1}$ ), whereas at least 0.2 mW are generated at the edges of the tuning range. At 7  $\mu\text{m}$  (1429  $\text{cm}^{-1}$ ), fluctuations of the central wavelength are measured to be 0.013% rms, whereas fluctuations of the FWHM bandwidth are as low as 0.61% rms. The wavelength stability is of great importance for FTIR spectroscopy, as the signal is typically derived by dividing a spectrum measured on the sample by a reference spectrum. Therefore minor spectral fluctuations can lead to significant signal noise, as discussed later.

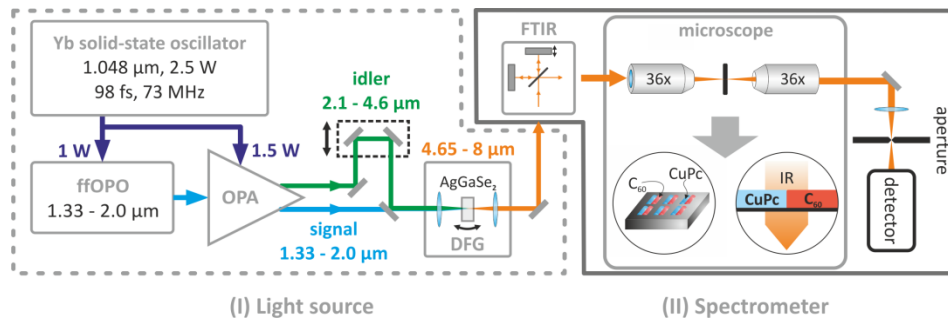


Fig. 1. Experimental setup. Mid-IR radiation is generated in a 2-mm-long AgGaSe<sub>2</sub> crystal by mixing signal and idler beams of a post-amplified fiber-feedback optical parametric oscillator (ffOPO) system, as presented in [22]. In contrast to [22], a commercial Yb solid-state laser with much shorter pulses and broader bandwidth is used for pumping, which provides 98 fs pulses at 73 MHz repetition rate and 1.048  $\mu\text{m}$  central wavelength. The DFG signal is coupled into a FTIR spectrometer and an attached microscope. A part of the microscope image is extracted by a quadratic aperture of area 10x10  $\mu\text{m}^2$  and detected by a MCT detector. Mid-IR molecular absorptions of 100 nm thick C<sub>60</sub> and Cu-Phthalocyanine films are investigated. For all measurements a 36x condenser and objective are used.

A spectrometer unit is attached to the laser, consisting of a Bruker Vertex 80 FTIR in combination with a Bruker Hyperion 2000 microscope. A MCT D313 detector is used to measure all spectra. According to the manufacturer it covers the spectral range between 850 – 12 000  $\text{cm}^{-1}$  and the sensitivity is  $D^* > 4 \times 10^{10} \text{ cm Hz}^{1/2} \text{ W}^{-1}$ . The FTIR also provides a built-in global, whose performance is used as a reference for the laser system.

A 36x objective and condenser are used to investigate the sample. This allows tight focusing, which enables higher spatial resolution, compared to the use of a 15x condenser and objective. The measured area, i.e. the spatial resolution, is defined by an adjustable aperture in front of the detector, as depicted in Fig. 1. It is set to  $10 \times 10 \mu\text{m}^2$ .

To account for dust and air flow, and to decrease atmospheric absorptions, the laser and microscope are housed and flushed with dry air. We want to point out that especially the laser box shows some leakage, due to connectors for the laser pump diode. In general, water absorptions could not be avoided completely.

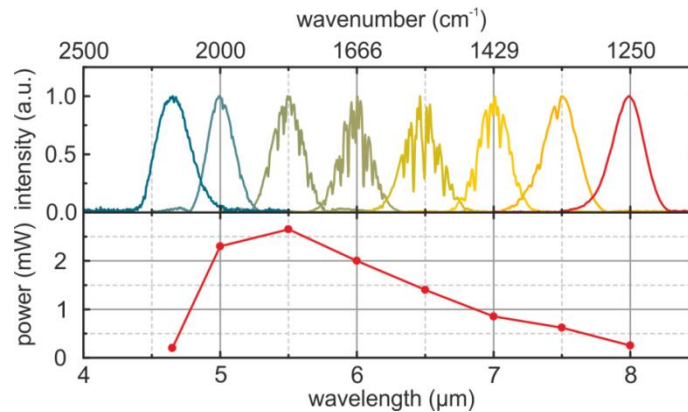


Fig. 2. Normalized spectra and output power over the DFG signal tuning range, spanning from 4.65 to 8  $\mu\text{m}$ . The spectral bandwidth (FWHM) reaches at least 250 nm over the whole tuning range. Up to 2.65 mW output power can be generated at 5.5  $\mu\text{m}$  wavelength, while 0.2 mW are available at the edges of the tuning range. Between 5 and 7  $\mu\text{m}$  wavelength, spectral features due to water absorption are visible on the spectral traces.

### 3. Experimental results

The measured sample consists of several 100 nm thick copper phthalocyanine (CuPc) and  $\text{C}_{60}$  layers, which are evaporated on a  $\text{CaF}_2$  substrate using stencil masks. To detect molecular vibrations in FTIR spectroscopy, a spectrum measured on the sample is divided by a reference spectrum of the bare light source. Thus spectral changes due to tiny absorptions become visible, superimposed onto an ideally flat 100% line. Therefore an excellent wavelength stability of the light source is required, as briefly explained in the following. Assuming two identical spectra are divided, their division will be a flat line of amplitude 1 or 100%. If one spectrum is spectrally shifted, this baseline will be tilted, whereas a change in intensity will lead to a baseline of different amplitude. In consequence, spectral and power fluctuations of the FTIR light source can lead to strong FTIR signal noise. In general, time-dependent fluctuations of the light source or changing atmospheric conditions during the measurements may result in a shift of the baseline.

#### 3.1 Sample characterization

Before mapping the sample with our laser source, it is characterized by applying the globar. For this characterization, a 15x condenser and objective are used, as the aperture size is set to  $100 \times 100 \mu\text{m}^2$  to investigate a sufficiently large sample area that contains both molecules. 200 spectra are averaged to achieve a reasonable signal-to-noise ratio. They are recorded at a spectral resolution of  $4 \text{ cm}^{-1}$ . Figure 3(a) depicts the characterization data in the range from 1350 to 1500  $\text{cm}^{-1}$  (7.4 – 6.67  $\mu\text{m}$ ). This frequency range is of interest, as both molecules exhibit vibrations that are close together and of similar magnitude. The resonances are found to be located at 1421  $\text{cm}^{-1}$  (CuPc) and 1429  $\text{cm}^{-1}$  ( $\text{C}_{60}$ ), respectively.

### 3.2 Laser-based FTIR mapping

In the following, a  $150 \times 150 \mu\text{m}^2$  sample area is mapped using our laser system. The aperture size is set to  $10 \times 10 \mu\text{m}^2$  and all spectra are measured at  $2 \text{ cm}^{-1}$  spectral resolution. Both vibrations can be addressed simultaneously by tuning the laser to  $1430 \text{ cm}^{-1}$  ( $7 \mu\text{m}$ ), as also illustrated in Fig. 3(a). Here, the laser reaches a FWHM of  $59 \text{ cm}^{-1}$  ( $289 \text{ nm}$ ). An average laser power of  $0.7 \text{ mW}$  is applied during the experiments.

For all measurements, a background spectrum is recorded on the bare  $\text{CaF}_2$  substrate, before measuring a sample spectrum on the molecule layers. On each pixel of the map 15 spectra are recorded and averaged. The sample and background spectra are measured alternately for that purpose. Thus measuring one pixel takes 143 sec. After a linear baseline correction within the FWHM bandwidth of the laser, the peak absorption of the respective molecule is evaluated. These values are displayed in the map at the corresponding pixel position, whereby a signal threshold of 0.25% is applied.

The measured sample area is shown in Fig. 3(b). Here, the CuPc layers appear blue, while the  $\text{C}_{60}$  layers are red. Figure 3(c) depicts the evaluated map, showing both molecules, which matches the microscope image very well. Again, CuPc appears blue, whereas  $\text{C}_{60}$  is colored red. Further details are visible in Figs. 3(d) and 3(e), which show the separated absorption maps of CuPc and  $\text{C}_{60}$ , respectively. The layers and the different molecules are well distinguishable and the contrast to the  $\text{CaF}_2$  substrate is high.

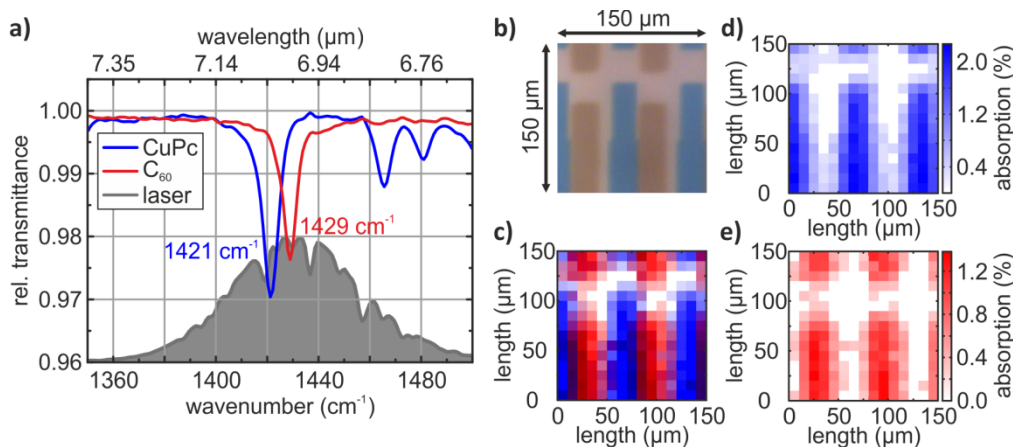


Fig. 3. a) Characterization spectra of the Cu-Phthalocyanine and  $\text{C}_{60}$  vibrations that are going to be investigated using the FTIR setup. These characterization spectra have been measured using the globar, with an aperture size of  $100 \times 100 \mu\text{m}^2$  and by averaging 200 spectra at  $4 \text{ cm}^{-1}$  spectral resolution. The grey spectrum depicts the laser spectrum that is used during the experiments. Due to a FWHM of the laser spectrum of  $59 \text{ cm}^{-1}$  ( $289 \text{ nm}$ ) both vibrations can be measured without adjusting the laser wavelength. b) Microscope image of the scanned  $150 \times 150 \mu\text{m}^2$  sample area that is investigated with the laser. c-e) Evaluated FTIR maps measured with the laser system. The strength of the molecular absorption of the respective vibration is depicted as a function of the position. The area is scanned with  $10 \times 10 \mu\text{m}^2$  resolution,  $4 \text{ cm}^{-1}$  spectral resolution, averaging 15 spectra per pixel, which corresponds to a pixel measurement time of 143 sec. Thus, both molecular features are well distinguishable. To visualize the overlap with the sample image (b), the color code of the maps matches the microscope image. Therefore the absorption of  $\text{C}_{60}$  is shown in red, whereas CuPc appears blue. Good overlap between the measured maps and the microscope image (b) is visible.

### 3.3 Comparing the laser system and the globar

To quantify the enhanced detection limit of laser-based FTIR spectroscopy, the previous measurements are repeated using the standard globar light source instead of the laser system. All measurement settings remained unchanged and the experiment has been conducted directly after the laser measurement to ensure similar conditions. The corresponding maps are

depicted in Fig. 4(a). Here, no molecular layers can be identified, due to the rather low global brilliance [10]. This leads to a high noise level, as too few photons hit the detector to overcome the detector noise. To decrease the noise, longer integration is needed, which would result in unacceptably long measurement times, as the current mapping already required 8 hours 56 minutes. At this point we would like to point out that there might be a different impact of water absorptions on the laser and global measurements, as particularly our laser box shows some leakage. The measured relative humidity inside the laser box has not been lower than 20%, whereas it has been on the order of 10% inside the micro-FTIR spectrometer.

Subsequently, the minimum number of averaged spectra required to detect the molecular resonances with the laser is investigated. Using the data from the previous laser-based mapping, at least 3 signal spectra need to be averaged to observe vibrational features. This corresponds to a measurement time of 29 sec per pixel, which corresponds to a scanning speed of  $3.5 \mu\text{m}/\text{sec}$ . Hence, a  $150 \times 150 \mu\text{m}^2$  map is estimated to require 109 minutes. Figure 4(b) illustrates the laser-based maps using 3 averaged signal spectra per pixel. In contrast to Figs. 3(d) and 3(e) absorption features below approximately 0.5% are covered by noise.

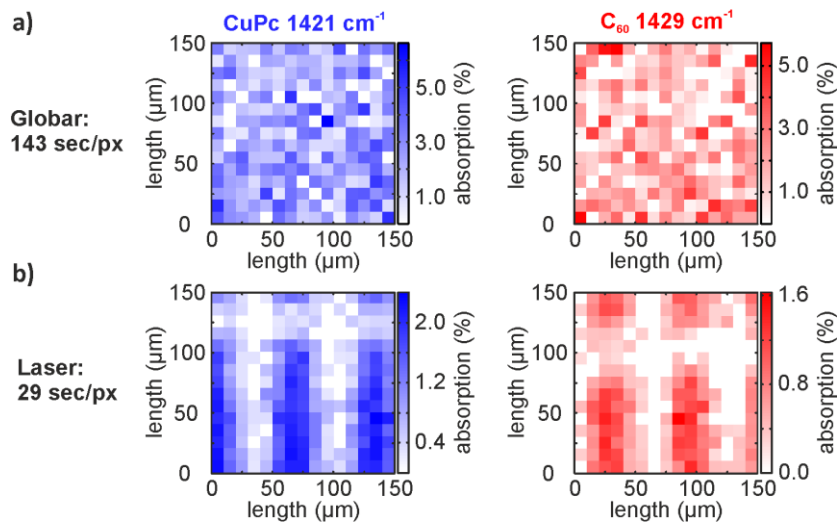


Fig. 4. Comparison between FTIR maps conducted using the global (a) and the laser (b) as light sources. Whereas no molecular features can be resolved using the global, high chemical contrast is achieved with the laser, even at a 5 times shorter integration time given in seconds per pixel (sec/px). Different scales between the global and laser maps are due to the higher noise level of the global.

### 3.4 Noise investigations

Finally, the noise level of the presented measurements is evaluated. For that purpose consecutive background spectra are divided and their rms deviation is calculated, thus reflecting the bare light source noise. This is conducted in the frequency range from  $1400$  to  $1460 \text{ cm}^{-1}$ , which corresponds to the FWHM bandwidth of the laser spectrum. The calculated rms fluctuations describe the noise level of the previously shown maps. Vibrational bands, whose absorption exceeds this noise level, can be measured with a single spectrum. Averaging of multiple measurements is required to detect other absorption signals that are below this noise floor. Figure 5(a) depicts the rms noise for both the laser and the global during 400 minutes. Here, the global noise shows an initial drift before it reaches its equilibrium performance. This drift can be thermally induced, as the global radiates heat. Furthermore the MCT detector has been refilled with liquid nitrogen, which also leads to a mechanical drift of the microscope due to the extra weight of the full detector. This effect is

expected to be rather small, as a box has been built around the microscope that also braces it. However, the combination of both issues is assumed to cause this initial drift, which is further investigated currently. No comparable drift is seen using the laser, which can be due to the low power of 0.7 mW, applied during the measurements. Thus a thermal drift due to the light source can be excluded. Nevertheless, the global noise reaches 6.41% rms in average, which exceeds the laser by more than one order of magnitude. The laser noise is as small as 0.47% rms, which matches the noise level visible in Fig. 4(b) of about 0.5% well. Figure 5(b) underlines these results, by depicting signal spectra of arbitrarily chosen measurement positions on the molecular layers, without having any baseline correction applied. The more than one order of magnitude higher noise level of the global compared to the laser is clearly visible. Despite averaging 15 signal spectra, which corresponds to a pixel measurement time of 143 sec, the molecular vibrations remain covered by noise. In contrast to this, the CuPc and C<sub>60</sub> resonances are distinctly visible for laser-based FTIR spectroscopy, even at a 5 times shorter measurement time of only 29 s per pixel.

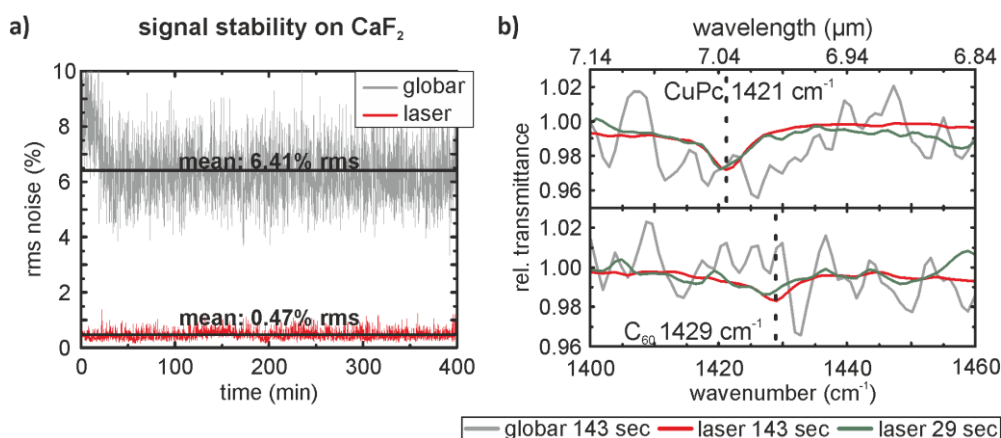


Fig. 5. a) Comparison of laser and global noise in the frequency range from 1400 to 1460 cm<sup>-1</sup>, which corresponds to the FWHM of the laser spectrum. About one order of magnitude higher rms noise is present when using the global during a period of 400 min. Both measurements have been extracted from the mappings depicted in Fig. 3 by comparing subsequent reference spectra measured on the CaF<sub>2</sub> substrate. Thus, the noise level gives a lower limit of detectable molecular absorptions without averaging multiple spectra. b) Comparison of FTIR signal spectra using the global and the laser, extracted from randomly chosen pixels (px 25 and px 37) of the maps that are displayed in Fig. 3. The global noise substantially exceeds the molecular absorptions, as expected from the noise level, as demonstrated in a). Even at short measurement times of 29 sec, both molecular absorptions remain distinctly visible using the laser. No baseline corrections have been applied on these spectra.

#### 4. Summary

In conclusion, by applying a broadband, low-noise and low-drift laser source that is continuously tunable from 1250 – 7520 cm<sup>-1</sup> (1.33 – 8 μm), the limits of FTIR spectroscopy in terms of measurable sample areas, measurement time and detection limit could be extended. Compared to a thermal light source, the detection limit is enhanced due to a more than one order of magnitude lower noise level. This allows a significant reduction of the measurement time and enables spatially resolved FTIR spectroscopy, as demonstrated by mapping a 150x150 μm<sup>2</sup> large area in only 109 minutes. This has not been possible employing a thermal light source, even at a total measurement of nearly 9 h.

By using a pump laser with higher average power, the laser tuning range could be extended up to 20 μm wavelength [23], which allows spectroscopy over the entire fingerprint region. Furthermore a broader FWHM bandwidth of the mid-IR pulses is expected by replacing the AgGaSe<sub>2</sub> crystal by a GaSe crystal, which exhibits broader phase-matching

bandwidth. This would simplify the detection of broader resonances such as plasmonic resonances or the detection of multiple and distinctly separated vibrational bands, as less tuning of the laser wavelength is required.

Due to the high sensitivity, low noise and simplicity, this tabletop system shows great potential for mid-IR spectroscopy. Considering the very low required intensities and the available average power from parametric sources, direct FTIR mapping using focal-plane arrays is feasible, which would greatly accelerate the acquisition of large scale samples. Complementary new applications such as FTIR measurements on single nanoparticles, which are on the order of the diffraction limit of the laser wavelength, or the detection of very low molecule concentrations become possible as well.

Currently this setup is applied to monitor protein folding processes in combination with surface-enhanced infrared absorption (SEIRA) [24–26] on single gold nanoantennas. Beside its far-field spectroscopy application, this system also shows huge potential for near-field spectroscopy using s-SNOM (scattering-type Scanning Near-field Optical Microscopy). State-of-the-art devices also use interferometric spectroscopy (nano FTIR), wherefore it would be interesting to transfer our system from the far-field to the near-field. Furthermore our laser system might be suited for such applications, due to its bandwidth, low noise, tuning range and long-term stability, as previous publications on mid-IR sources for s-SNOM have indicated [27–29]. The laser system might ultimately even enable a low-noise mid-infrared femtosecond pump-probe configurations.

### Funding

European Research Council (ERC) (COMPLEXPLAS); Baden-Württemberg Stiftung (PROTEINSENS, Spitzenforschung II); Carl-Zeiss Stiftung; Bundesministerium für Bildung und Forschung (BMBF); Deutsche Forschungsgemeinschaft (DFG) (SPP1839).